

## Preparation, characterization and reactivity of Pd/Nb<sub>2</sub>O<sub>5</sub> catalysts in hexa-1,5-diene hydrogenation

Roberta Brayner<sup>a,b,\*</sup>, Guillaume Viau<sup>a</sup>, Gilberto M. da Cruz<sup>b</sup>, Françoise Fiévet-Vincent<sup>a</sup>,  
Fernand Fiévet<sup>a</sup>, François Bozon-Verduraz<sup>a</sup>

<sup>a</sup> Laboratoire de Chimie des Matériaux Divisés et Catalyse, Université Paris 7, 2 Place Jussieu, 75251 Paris Cedex 05, France

<sup>b</sup> Departamento de Engenharia de Materiais, Faculdade de Engenharia Química de Lorena Rod. Itajuba-Lorena,  
Km 74.5 12600-000 Lorena SP, Brazil

### Abstract

Palladium/niobia catalysts are prepared by various methods involving either gas or liquid phase reduction. Although giving rise to average or low dispersion, the reduction of palladium precursors in a liquid medium (hydrazine or ethylene-glycol) appears to be a promising method since a low dispersion favors the activity in the hydrogenation of hexa-1,5-diene in liquid phase. The substitution of alumina by niobia improves the fractional selectivity and the yield of hex-1-ene in all cases. A very good global selectivity is also observed. ©2000 Elsevier Science B.V. All rights reserved.

**Keywords:** Hexa-1,5-diene; Liquid phase hydrogenation; Palladium/niobia catalysts; Polyol process; Diffuse reflectance

### 1. Introduction

Niobia-supported metal catalysts have attracted little attention even though a growing interest is now observed [5,6]. The aim of this work is to study the different factors influencing the reactivity of niobia-supported palladium catalysts by varying (i) the thermal treatments of niobia, and (ii) the preparation mode of the catalyst and especially the activating (reducing) treatment. The samples are characterized after the different preparation stages. The test reaction is the selective hydrogenation of hexa-1,5-diene, which has received little attention despite its interest as model reaction for hydrogenation of the undesirable C<sub>11</sub>–C<sub>13</sub> alkadienes to alkenes used in the linear alkyl-benzene production [8]. The performances of Pd/niobia catalysts will be compared with those of Pd/alumina.

### 2. Experimental

Nb<sub>2</sub>O<sub>5</sub> (HY-340) was kindly supplied by CBMM (Companhia Brasileira de Metalurgia e Mineração, Brazil) and palladium salts were obtained from Engelhard, France.

Three methods of preparation were employed: (i) the *anchoring method* was achieved as follows; first Pd acetylacetonate was anchored [7] on niobia from a solution in toluene at 383 K for 5 h (A<sub>1</sub>), at 383 K for 2 h (A<sub>2</sub>) and at 333 K for 2 h (A<sub>3</sub>); the solids obtained after filtering and washing by toluene at room temperature were dried at 323 K overnight and calcined for 6 h under flowing oxygen either at 673 K (A<sub>1</sub>-C and A<sub>3</sub>-C) or at 573 K (A<sub>2</sub>-C). Secondly, the calcined samples were reduced either in flowing 10% H<sub>2</sub>/He (A<sub>1</sub>-CH<sub>1</sub> at 473 K and A<sub>2</sub>-CH<sub>2</sub> at 343 K) or in a liquid medium: hydrazine at 273 K (A<sub>3</sub>-CHZ<sub>2</sub>) and ethylene-glycol (EG) at 343 K (A<sub>3</sub>-CEG<sub>2</sub>); (ii) in the “*polyol method*” [3,9], the catalysts were obtained through direct

\* Corresponding author.

reduction at room temperature of palladium nitrate by EG in a suspension of niobia calcined at 773 K (EG<sub>1</sub>); (iii) in the *hydrazine method*, direct reduction of Pd acetylacetonate anchored on niobia was performed in a 10% hydrazine solution [4] at 273 K (A<sub>2</sub>-HZ<sub>1</sub>).

The reduction methods and the characteristics of the final samples are summarized in Table 1.

Chemical analyses were carried out at the Materials Engineering Department, DEMAR/FAENQUIL, Lorena SP, Brazil by inductively coupling plasma atomic emission spectroscopy (ICP-AES).

X-ray powder diffraction (XRD) patterns were recorded using Co K $\alpha$  radiation. The diffractometer was calibrated using a standard Si sample. The counting time was 30 s per step ( $2\theta$ ) of 0.05°. The mean crystallite size was estimated using the Scherrer equation, after computer fitting using pseudo-Voigt function (software Profile, SOCRABIM Diffract-At).

TEM measurements were performed with a JEOL 100 CXII microscope operating at 100 kV. The particle size distribution was obtained from the TEM pictures using a digital camera and the SAISAM and TAMIS software (Microvision Instruments), calculating the surface-average particle diameter from  $d_p = \sum n_i d_i^2 / \sum n_i d_i$ .

UV-Vis-NIR diffuse reflectance spectra (DRS) were recorded on a Cary 5E spectrophotometer equipped with an integration sphere coated with PTFE.

The catalytic tests were performed in a 100 ml well stirred three phase slurry type thermoregulated glass reactor filled with 50 ml of 2 wt.% hexa-1,5-diene in heptane solution. The catalysts (30 mg) were first outgassed for 1 h in the reactor, before treatment with 792 Torr hydrogen at 313 K for 1 h, this procedure was repeated with a final outgassing before introduction of the reaction medium containing the reagent,

hexa-1,5-diene, the internal standard, *n*-pentane (around 1 wt.%), and the solvent, *n*-heptane, already saturated with hydrogen. The hydrogen was charged up to the operating pressure, 792 Torr, while the first analysis sample was collected, and stirring was begun (2000 rpm).

The reaction was carried out at constant pressure, hydrogen being supplied from a thermostated vessel, acting as a reservoir, filled initially with 980 Torr of this gas.

During the reaction, small liquid samples were collected through a syringe valve equipped with a microfilter, at regular H<sub>2</sub> uptake intervals, to follow the changes of the reaction medium composition.

A Delsi Di200 gas chromatograph (GC) using a flame ionization detector (FID) was used to analyze the liquid samples collected during the reaction. The reagent, hexa-1,5-diene, the internal standard *n*-pentane, the solvent, *n*-heptane and the products (hexane, hex-1-ene, E,Z-hex-2-ene and E,Z-hex-3-ene) were separated on a 50 m, 0.2 mm HP PONA capillary column.

The use of standards during the gas chromatography analysis allowed the measurement of the concentration of the reactant and of the products. The formation of other possible byproducts was not detected.

### 3. Results and discussion

#### 3.1. Characterization of catalysts

Table 1 collects the characteristics of the samples prepared.

The DR spectrum of pure Nb<sub>2</sub>O<sub>5</sub> (Fig. 1) calcined at different temperatures (573, 673 and 773 K) is characterized by a strong absorption in the UV range due

Table 1  
Characteristics of the samples

Sample	Support calcination temperature (K)	Reduction method	Pd (%)	Mean particle size (nm) (TEM)	Mean crystallite size (nm) (XRD)
A <sub>1</sub> -CH <sub>1</sub>	673	Under flowing 10 wt.% H <sub>2</sub> /He at 473 K for 2 h	3.2	2.7	3.2
A <sub>2</sub> -CH <sub>2</sub>	573	Under flowing 10 wt.% H <sub>2</sub> /He at 343 K for 2 h	2.5	6.2	7.8
A <sub>2</sub> -HZ <sub>1</sub>	573	In hydrazine solution at 273 K for 5 min	2.5	5.2	5.3
A <sub>3</sub> -CHZ <sub>2</sub>	673	In hydrazine solution at 273 K for 5 min	1.3	3.0	5.5
EG <sub>1</sub>	773	EG at 273 K for 24 h	4.0	6.0	6.3
A <sub>3</sub> -CEG <sub>2</sub>	673	EG at 343 K for 3 h	1.3	5.1	6.7

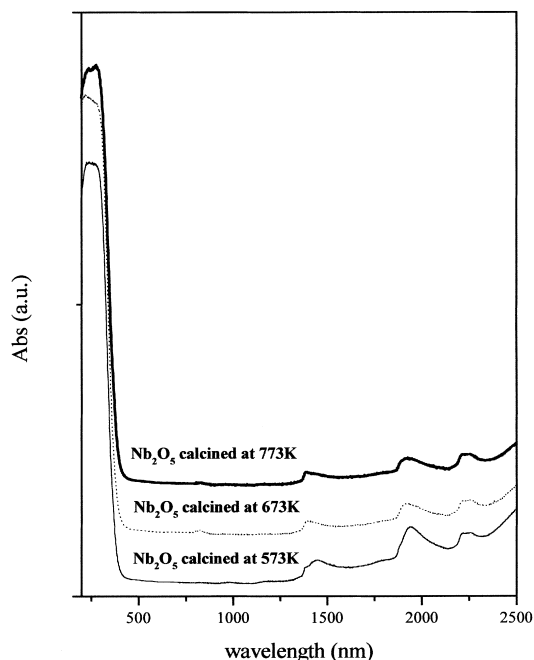


Fig. 1. DR spectra of pure  $\text{Nb}_2\text{O}_5$  calcined at 573, 673 and 773 K for 6 h.

to the interband transition and allows the estimation of the band gap width (3.4 eV, absorption threshold near 360 nm). The NIR range presents also harmonics and combination bands of OH groups whose intensity depends on the calcination temperature (Fig. 1). The DRS of  $A_3$  after anchoring (Fig. 2) shows a shoulder near 445 nm due to d–d transitions of  $\text{Pd}(\text{acac})_2$  [7]. After heating in flowing  $\text{O}_2$  at 673 K, the shoulder near 445 nm is shifted to 490 nm (Fig. 3,  $A_3$ -C). This can be ascribed to the formation of isolated  $\text{Pd}^{2+}$  ions or of small palladium–oxygen entities and not to bulk PdO particles, whose absorption threshold lies in the NIR [7]. On the other hand, the samples  $A_1$  and  $A_2$  showed background absorption increasing from the NIR to the visible range (Fig. 2), characteristic of metallic particles [2,7]; whereas the d–d transitions of  $\text{Pd}(\text{acac})_2$  (see above) are not observed, showing that this metal complex was, at least partially, reduced on niobia during the anchoring process at 383 K. The increasing background is also observed for  $A_2$ -C sample (Fig. 3) after calcination at 573 K, showing that this temperature is not high enough to achieve complete oxidation of metal par-

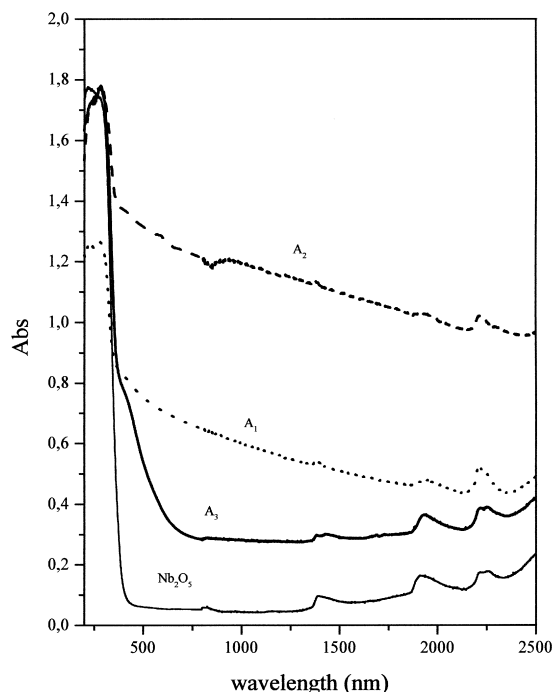


Fig. 2. DR spectra of the samples  $A_1$ ,  $A_2$  and  $A_3$  after anchoring.

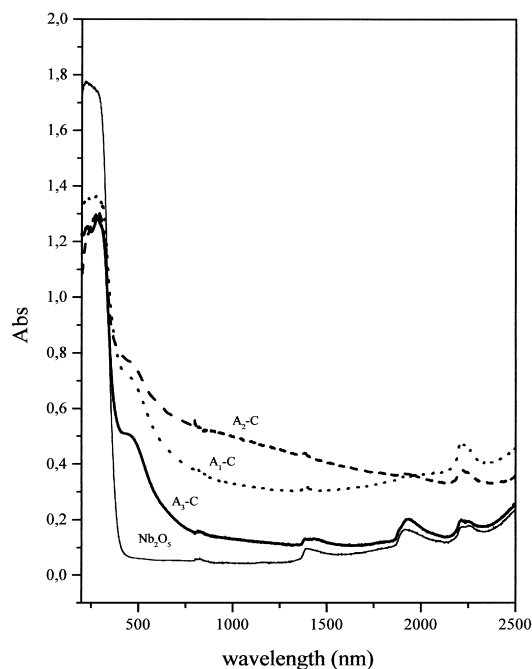


Fig. 3. DR spectra of the samples  $A_1$ -C,  $A_2$ -C and  $A_3$ -C after calcination under flowing  $\text{O}_2$  for 6 h.

ticles. The XRD patterns confirm the DRS results, i.e. (i) the formation of  $\text{Pd}^0$  on  $\text{A}_1$  and  $\text{A}_2$  samples *after anchoring*; (ii) the presence of  $\text{Pd}^0$  in the  $\text{A}_2\text{-C}$  sample.

Table 1 shows a good agreement between the particle size inferred from TEM image analysis and the crystallite size inferred from the X-ray line broadening. The smallest particle sizes are obtained when (i) the calcination temperature of the support is high ( $\text{A}_1\text{-CH}_1$ ,  $\text{A}_3\text{-CHZ}_2$ ); (ii) the reduction is carried out in the gas phase. Fig. 4 shows the particle size distribution of  $\text{A}_1\text{-CH}_1$  and  $\text{EG}_1$  samples. Sample  $\text{A}_1\text{-CH}_1$ , reduced in gas phase, shows nanoparticles with a narrow size distribution; on the other hand, reduction in liquid polyol ( $\text{EG}_1$ ) leads to particles with a broader size distribution. This can be explained by an incomplete separation of the nucleation and

growth steps of the particles from the solution and/or a coalescence of the particles during the growth step. This last phenomenon is still more noticeable for sample  $\text{A}_2\text{-HZ}_1$  prepared by reduction in solution by the hydrazine method (large size distribution, not shown).

### 3.2. Reactivity in hexa-1,5-diene

The thermodynamic order of stability of the alkene isomers is:  $\text{Z-hex-2-ene} > \text{E-hex-2-ene} > \text{E-hex-3-ene} > \text{Z-hex-3-ene} > \text{hex-1-ene}$  [8]. The selectivity values are expressed by (i) the *global selectivity* (percentage of hexadiene converted in hexenes); (ii) the *fractional selectivity* to hex-1-ene (proportion of this isomer among all hexenes), product chosen as a target, as the least thermodynamically favored.

The performances of the catalysts differ markedly (Figs. 5–7 and Table 2). Whereas all catalysts present a very good *global selectivity*  $S_g$  (Table 2), their activity show significant disparities; the well dispersed samples ( $\text{A}_1\text{-CH}_1$  and  $\text{A}_3\text{-CHZ}_2$ ) are less active than the samples with low dispersion ( $\text{A}_2\text{-CH}_2$ ,  $\text{EG}_1$ ,

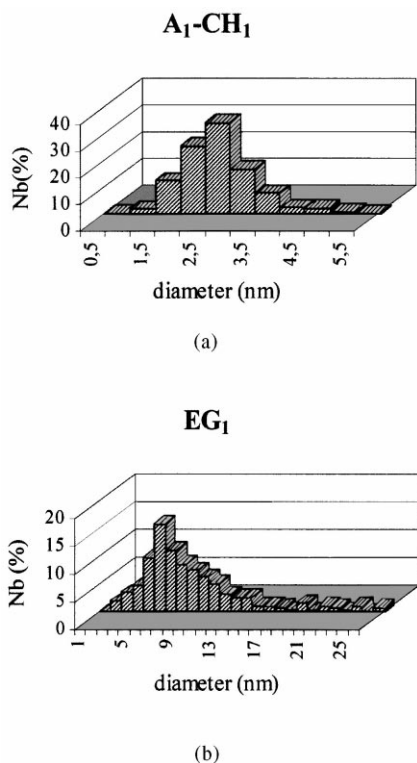


Fig. 4. (a) Particle size distribution of  $\text{A}_1\text{-CH}_1$  sample after reduction under flowing 10%  $\text{H}_2/\text{He}$  at 473 K. (b) Particle size distribution of  $\text{EG}_1$  sample after reduction in ethylene-glycol at room temperature.

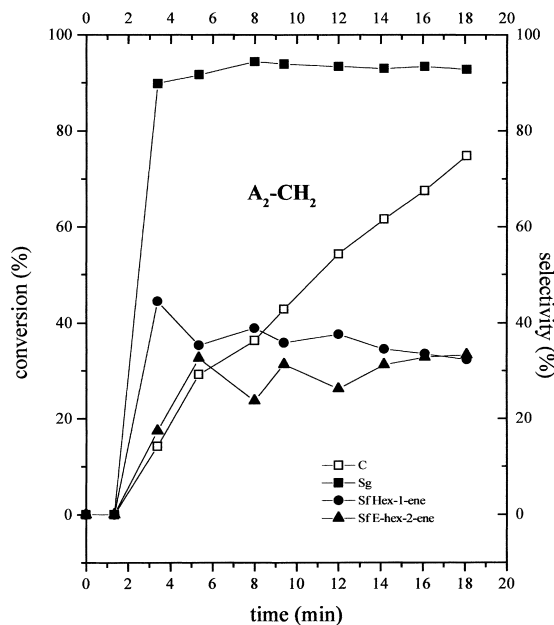


Fig. 5. Global ( $S_g$ ) and fractional ( $S_f$ ) selectivities and conversion (C) versus time:  $\text{A}_2\text{-CH}_2$  sample.

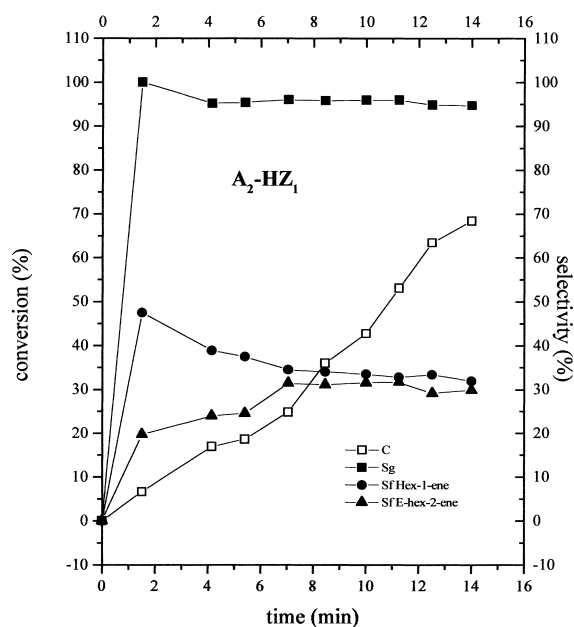


Fig. 6. Global ( $S_g$ ) and fractional ( $S_f$ ) selectivities and conversion (C) versus time: A<sub>2</sub>-HZ<sub>1</sub> sample.

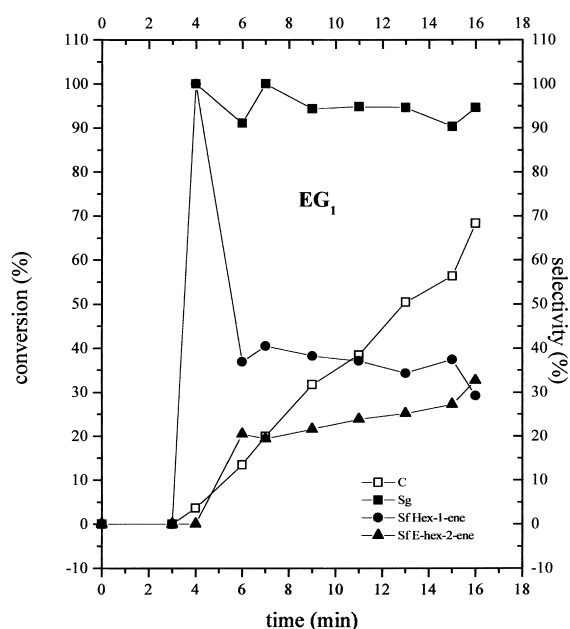


Fig. 7. Global ( $S_g$ ) and fractional ( $S_f$ ) selectivities and conversion (C) versus time: EG<sub>1</sub> sample.

A<sub>3</sub>-CEG<sub>2</sub> and A<sub>2</sub>-HZ<sub>1</sub>); sample A<sub>2</sub>-HZ<sub>1</sub> is as active as Pd/alumina [8] but shows a much better fractional selectivity  $S_f$  to hex-1-ene. For all catalysts,  $S_f$  is greater than 50% at low conversion then it decreases, because isomerization to hex-2-enes occurs, and remains nearly constant at high conversion. The catalysts reduced in ethylene-glycol (EG<sub>1</sub> and A<sub>3</sub>-CEG<sub>2</sub>) exhibit also good performances, A<sub>3</sub>-CEG<sub>2</sub> showing the highest value of  $S_f$ , two times higher than the Pd/Al<sub>2</sub>O<sub>3</sub> catalyst prepared by polyol method [8]. It

appears that the best performances result from a compromise between the number of sites and their activity which itself depends on the particle size; if, indeed, the particle size is small, the co-ordination unsaturation is high; hence the adsorption of dienes is strong, which decreases the site activity; on the other hand, on large particles the reaction occurs mainly on sites of higher co-ordination (low unsaturation). Similar results were previously reported in the hydrogenation of but-1-yne or butadienes in the liquid phase [1].

Table 2  
Catalytic results

Catalyst	Pd (%)	FME	$V_s(\text{mol s}^{-1} \text{g}_{\text{Pd}}^{-1})^a$	Reaction time (min)	C (%)	$S_g$ (%)
A <sub>1</sub> -CH <sub>1</sub>	3.2	0.33	$2.0 \times 10^{-3}$	70	72	95
A <sub>2</sub> -CH <sub>2</sub>	2.5	0.15	$1.02 \times 10^{-2}$	18	75	93
EG <sub>1</sub> <sup>b</sup>	4.0	0.15	$9.0 \times 10^{-3}$	15	57	91
A <sub>3</sub> -CEG <sub>2</sub>	1.3	0.18	$1.0 \times 10^{-2}$	39	68	95
A <sub>2</sub> -HZ <sub>1</sub>	2.5	0.17	$1.5 \times 10^{-2}$	14	69	95
A <sub>3</sub> -CHZ <sub>2</sub>	1.3	0.30	$4.6 \times 10^{-3}$	68	53	95
Pd/Al <sub>2</sub> O <sub>3</sub> <sup>b</sup>	10.0	0.13	$1.4 \times 10^{-2}$	15	92	85

<sup>a</sup>  $V_s$ , activity (initial rate). The mass of catalysts varied from 15 to 30 mg.

<sup>b</sup> Polyol method.

#### 4. Conclusion

The preparation methods presented in this work have led to contrasted results; although it gives rise to average or low dispersion, the reduction of palladium precursors in a liquid medium (hydrazine or ethylene-glycol) appears to be a promising method. Concerning the hydrogenation of hexa-1,5-diene in the liquid phase, the substitution of alumina by niobia improves the fractional selectivity and the yield in hex-1-ene in all cases and a very good global selectivity is also observed.

A better control of the palladium size and distribution is now under study and involves an increase of the support calcination temperature, as well as a decrease of the anchoring temperature and of the duration of the reduction processes.

#### Acknowledgements

The authors are indebted to CNPq, Brazil for support and financial resources.

Thanks to J.R. Barbosa (Materials Engineering Department, DEMAR/FAENQUIL, Lorena SP, Brazil)

for the ICP-AES analysis and to Dr. E.A. Sales (Federal University of Bahia, Brazil) for his initial help in catalytic measurements optimization.

The authors are grateful to M.J. Vaulay and G. Cheguillaume for their technical assistance.

#### References

- [1] J.P. Boitiaux, J. Cosyns, S. Vasudevan, *Stud. Surf. Sci. Catal.* 16 (1983) 123.
- [2] J.A. Creighton, D.G. Eadon, *J. Chem. Soc., Faraday Trans.* 87 (1991) 3881.
- [3] F. Fiévet, J.P. Lagier, M. Figlarz, *MRS Bull.* 14 (1989) 29.
- [4] L. Filotti, A. Bensalem, F. Bozon-Verduraz, G.A. Shafeev, V.V. Voronov, *Appl. Surf. Sci.* 109/110 (1997) 249.
- [5] F.B. Passos, D.A.G. Aranda, R.R. Soares, M. Schmal, *Catal. Today* 43 (1998) 3.
- [6] M.M. Pereira, F.B. Noronha, M. Schmal, *Catal. Today* 16 (1993) 407.
- [7] A. Rakai, D. Tessier, F. Bozon-Verduraz, *New J. Chem.* 16 (1992) 869.
- [8] E.A. Sales, B. Benhamida, V. Caizergues, J.P. Lagier, F. Fiévet, F. Bozon-Verduraz, *Appl. Catal. A* 172 (1998) 273.
- [9] G. Viau, F. Fiévet-Vincent, F. Fiévet, *J. Mater. Chem.* 6 (1996) 1047.